Journal of Power Sources 195 (2010) 307–312

Contents lists available at ScienceDirect

Journal of Power Sources

journal homepage: www.elsevier.com/locate/jpowsour

Promoted hydrogen generation from ammonia borane aqueous solution using cobalt–molybdenum–boron/nickel foam catalyst

Hong-Bin Dai, Li-Li Gao, Yan Liang, Xiang-Dong Kang, Ping Wang*

Shenyang National Laboratory for Materials Science, Institute of Metal Research, Chinese Academy of Sciences, 72 Wenhua Road, Shenyang 110016, PR China

ARTICLE INFO

Article history:
Received 23 March 2009
Received in revised form 23 June 2009
Accepted 30 June 2009
Available online 7 July 2009

Keywords:
Hydrogen generation
Ammonia borane
Electroless plating
Cobalt–molybdenum–boron/nickel foam catalyst
Hydrolysis kinetics

ABSTRACT

Ammonia borane (AB) is an intriguing molecular crystal with extremely high hydrogen density. In the present study, by using a modified electroless plating method, we prepare a robust supported cobalt–molybdenum–boron (Co–Mo–B)/nickel (Ni) foam catalyst that can effectively promote the hydrogen release from AB aqueous solution at ambient temperatures. The catalytic activity of the catalyst towards the hydrolysis reaction of AB can be further improved by appropriate calcination treatment. In an effort to understand the effect of calcination treatment on the catalytic activity of the catalyst, combined structural/phase analyses of the series of catalyst samples have been carried out. Using the catalyst that is calcined at optimized condition, a detailed study of the catalytic hydrolysis kinetics of AB is carried out. It is found that the hydrolysis of AB in the presence of Co–Mo–B/Ni foam catalyst follows first-order kinetics with respect to AB concentration and catalyst amount, respectively. The apparent activation energy of the catalyzed hydrolysis reaction is determined to be 44.3 kJ mol^{-1}, which compares favorably with the literature results for using other non-noble transition metal catalysts.

1. Introduction

The rising concerns over dwindling resources and the environmental impact of burning fossil fuels have triggered intensive attention on the usage of hydrogen as an alternative energy carrier. One of the major obstacles to the development of hydrogen-powered vehicles is the lack of safe and efficient means for on-board hydrogen storage [1,2]. Recently, ammonia borane (H_3NBH_3, AB) attracts considerable interest as a potential hydrogen storage medium [3–6]. AB is a colorless molecular crystal at room temperature, with a theoretical hydrogen density of 19.6 wt.% and 0.16 kg H_2 l^{-1} on the weight and volume bases, respectively. Hydrogen generation (HG) from AB and its adducts can proceed via various means. In 2006, Chandra and Xu reported the first experimental study of catalytic hydrolysis of AB by using metal catalysts [7]. Compared to solid phase thermolysis [8–11] and catalytic dehydrocoupling in non-aqueous solutions [12–14], catalytic hydrolysis of AB provides an alternative means for portable or transportational hydrogen storage/generation applications, as it allows on-demand generation of large amount of hydrogen at ambient temperatures.

AB is stable in air, and soluble in water with a solubility of 33.6 g AB/100 g water at room temperature. An important advantage of AB over other chemical hydrides [e.g. sodium borohydride ($NaBH_4$)] [15] is that the aqueous solution of AB is highly stable under inert atmosphere [16], thus eliminating the need of alkaline stabilizer. The hydrolysis reaction of AB following Eq. (1) can be

$$NH_3BH_3 + 2H_2O \xrightarrow{\text{Catalyst}} NH_4^+ + BO_2^- + 3H_2 \uparrow \quad (1)$$

accelerated by using catalysts. Besides acids accelerators [17], a number of transition metals (TM) or their alloys have been identified to be catalytically active towards the hydrolysis reaction of AB, including Rh, Pt, Ru, Ir, Pd [18–22], Ni–Pt alloy [23], Ni–Ag alloy [24], Fe [25], Co, Ni [26] and Cu [27,28], etc. The noble TM catalysts typically show excellent catalytic activities, but get restricted in most practical applications by the high material cost. Many recent efforts have been directed to the development of the cost-effective non-noble TM catalyst [22,25–28]. In particular, the supported non-noble TM catalysts are highly appreciated in the practical applications owing to their easy separation from fuel solution, and consequently the ready controllability of the hydrolysis reaction and reusability of the catalysts.

Several methods have been developed for preparation of supported non-noble TM catalysts, e.g. electroplating [29], electroless plating (EP) [29,30], dip-coating [31], and pulsed laser deposition [32]. Among these methods, EP is clearly the most popular and efficient one. EP of metal is an important industrial technique for metallizing insulators and objects with geometries that are difficult to coat by electroplating. In our recent study of $NaBH_4$-based chemical hydrogen storage system, we developed a modified EP method for preparation of supported TM catalyst [33,34]. Compared to the

* Corresponding author. Tel.: +86 24 2397 1622; fax: +86 24 2389 1320.
E-mail address: pingwang@imr.ac.cn (P. Wang).

0378-7753/$ – see front matter © 2009 Elsevier B.V. All rights reserved.
doi:10.1016/j.jpowsour.2009.06.094

conventional EP method, the newly developed technology is more efficient and capable of producing catalysts with much higher catalytic activity. For example, employing the Co–B/Ni foam catalyst prepared by the modified EP method in a 20 wt.% $NaBH_4$ + 10 wt.% NaOH solution yielded a HG rate of 11 l(min g)$^{-1}$ (Co–B), over six times higher than that obtained using the catalyst prepared by conventional EP method.

Quite recently, we further extended our study of chemical hydrides to AB. It has been found that the non-noble TM catalysts prepared by the modified EP method are also highly effective for promoting the hydrolysis reaction of AB. In this paper, we report the study results of catalytic hydrolysis of AB in the presence of the Co–Mo–B/Ni foam catalyst. The demonstrated high HG rate at ambient temperatures and prompt transient response, together with the inherent merits of chemical hydrides, make the catalyzed AB hydrolysis system promising for portable hydrogen storage/generation applications.

2. Experimental

2.1. Catalysts preparation and calcination treatment

The preparation of Co–Mo–B/Ni foam catalyst by the modified EP method involved the usage of solutions A and B with compositions given in Table 1. All the chemical reagents are of analytical grade and were used as received. Ni foam was selected as the catalyst support material due to its porous structure, low density, and high thermal and chemical stability under the hydrolysis conditions. The Ni foam (INCO ATM, 1.80 mm in thickness, 99.9% purity) has a network structure with an area density around 57.5 mg cm^{-2}, and an average pore size of 0.10–0.30 mm.

The Co–Mo–B/Ni foam catalyst was prepared following the procedure detailed in Refs. [33,34]. The chemical reactions involved in the EP process can be described as Eqs. (2)–(5).

$$BH_4^- + 2Co^{2+} + 4OH^- \rightarrow BO_2^- + 2Co\downarrow + 2H_2\uparrow + 2H_2O \quad (2)$$

$$3BH_4^- + 2MoO_4^{2-} + 2H_2O \rightarrow 3BO_2^- + 2Mo\downarrow + 6H_2\uparrow + 4OH^- \quad (3)$$

$$2BH_4^- + 2H_2O \rightarrow 2B\downarrow + 2OH^- + 5H_2\uparrow \quad (4)$$

$$BH_4^- + 2H_2O \rightarrow BO_2^- + 4H_2\uparrow \quad (5)$$

The EP process was repeated for two times to obtain a catalyst (Co–Mo–B) loading of around 16 mg cm^{-2} (Ni foam), as determined by the weight change before and after plating. The as-prepared Co–Mo–B/Ni foam catalyst was calcined at a temperature ranging from 250 to 500 °C for 2 h under Ar (99.999% purity) atmosphere. The applied heating rate is 2 °C min^{-1}.

Table 1
Bath compositions in preparation of the Co–Mo–B/Ni foam catalyst using the modified electroless plating method.

Bath solutions	Chemicals	Concentration (g l^{-1})
Solution A	$CoCl_2{\cdot}6H_2O$	50
	$Na_2MoO_4{\cdot}2H_2O$	12
	NH_4Cl	50
	$NH_3{\cdot}H_2O$ (ml l^{-1})	45
Solution B	$NaBH_4$	40
	NaOH	10

Note: the Ni foam is plated for two times at 25 °C.

2.2. Catalyst characterization

The Co–Mo–B/Ni foam catalysts were characterized by powder X-ray diffraction (PXRD, Rigaku D/MAX-2500, Cu Kα radiation) and scanning electron microscope (SEM, LEO Supra 35) equipped with energy dispersive X-ray (EDX) analysis unit (Oxford). The specific surface areas of the catalyst samples were measured by N_2 adsorption at 77 K using the Brunauer–Emmett–Teller (BET) method (Micromeritics ASAP 2010). To minimize the measurement error, each sample was measured for three times. The composition of the catalyst was analyzed by inductively coupled plasma-atomic emission spectrometry (ICP-AES, Iris Intrepid). The phase transformation behavior of the catalyst samples was examined by differential scanning calorimetry (DSC, Netzsch 449C) under flowing Ar (99.999% purity) atmosphere. The ramping rate is 10 °C min^{-1}.

2.3. Hydrolysis kinetics measurement

AB was synthesized by the reaction of $(NH_4)_2CO_3$ and $NaBH_4$ in a tetrahydrofuran solution following a literature procedure [35]. The purity of AB (~95%) was verified by X-ray diffraction measurements, elemental analyses and solid state ^{11}B NMR studies. The hydrolysis kinetics of AB was measured using a classic water-displacement method. The flask reactor containing the AB aqueous solution was placed in a thermostat that was equipped with a water circulating system to minimize the temperature rise resulting from the highly exothermic hydrolysis reaction. In a typical measurement, about 10 ml aqueous solution containing 1 wt.% AB was preheated and held at a designated temperature, and then one piece of the Co–Mo–B/Ni foam catalysts (1 cm × 1 cm) attracted on a magnetic stirring bar was dropped into the AB solution to initiate HG. During the measurements, the solution temperature was measured and carefully controlled within ±2 °C by adding ice-water blend. The volume of the generated hydrogen was measured by monitoring the water displaced from a graduated burette as the reaction processed. In the cyclic hydrolysis experiments, the post-used catalyst was washed thoroughly with deionized water and then reused.

3. Results and discussion

The supported Co–Mo–B/Ni foam catalyst can be readily prepared by using the modified EP method. Fig. 1 presents SEM morphologies of the as-prepared Co–Mo–B/Ni foam catalysts at the different magnifications and that calcined 350 °C after ten times of cyclic usage. After repeating the EP process for two times, the Ni foam surface (in Fig. 1a and b) was completely covered by the catalyst layer composed of Co, Mo and B elements, as indicated by the EDX analysis in Fig. 1e. Quantitative elemental analysis using ICP-AES determined that the catalyst layer contains 76.3 wt.% Co, 17.7 wt.% Mo and 6.0 wt.% B, corresponding to a formula of $Co_7Mo_1B_3$. It is notable that there exist some micro-cracks in the catalyst layer. Presumably, the generation of micro-cracks should be associated with the vigorous hydrogen evolution, and the relaxation of residual internal-stress resulting from the high nucleation and growth rates of the catalyst species during the modified EP process [30,36]. SEM examinations found that the supported catalyst is robust enough to retain its morphological feature after ten times of usage, as seen from the comparison between Fig. 1b and d. This is consistent with the observed cyclic stability of the catalytic activity of the catalyst (as stated below). The three-dimensional network structure of the Co–Mo–B/Ni foam catalyst allows the full access of reactants to the surface active sites of the catalyst, thereby ensuring a favorable catalytic performance from a structural point of view.

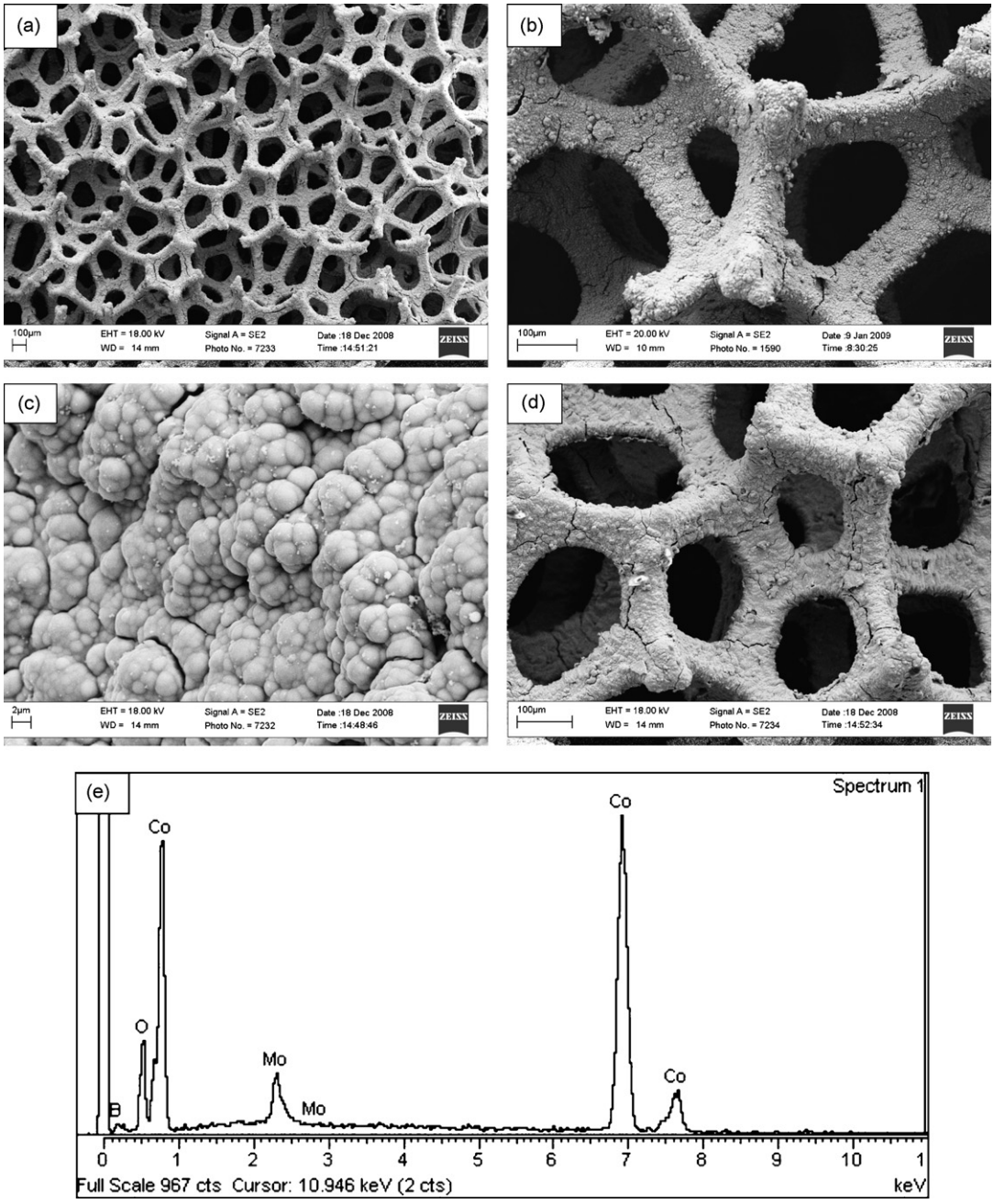

Fig. 1. SEM morphologies of the as-prepared Co–Mo–B/Ni foam catalysts at low (a), (b) and high (c) magnifications, and that calcined 350 °C after 10 times of cyclic usage (d). A representative EDX result of the catalyst sample is shown in (e).

Thus-prepared Co–Mo–B/Ni foam catalyst exhibits considerable catalytic activity towards the hydrolysis reaction of AB. As seen in Fig. 2a, the hydrolysis reaction of AB shows no induction period in the presence of the Co–Mo–B/Ni foam catalyst. The hydrogen release from 10 ml aqueous solution containing 1 wt.% AB amounts to 224 ml within 35 min at room temperature. This value corresponds to 2.85 out of a theoretical 3.0 equivalent H_2 following Eq. (1).

Further study found that the catalytic activity of the Co–Mo–B/Ni foam catalyst can be enhanced by appropriate calcination treatment. For example, calcination of the catalyst sample at 250 °C for 2 h under Ar atmosphere results in an around 20% increase on the average HG rate (Fig. 2b). Upon elevating the calcination temperature to 350 °C, the post-calcined catalyst enabled the hydrolysis reaction to be largely completed within 20 min (Fig. 2c), with an average HG rate nearly double that obtained using the as-prepared catalyst. But further increasing the calcination temperature, e.g. to 500 °C (Fig. 2d), resulted in a lowered catalytic activity of the catalyst. Here, it is noticed that variation of the calcination temperature affects the catalytic activity of the catalyst. But in all cases, around 100% conversion of AB is obtained upon extending the reaction time, depending upon the applied calcination condition of the catalyst.

In our preliminary efforts to understand the effect of calcination treatment on the catalytic activity, we performed combined structural/phase analyses of the series of the catalyst samples. Fig. 3 presents the XRD patterns of the as-prepared catalyst and those after being calcined at the varied temperatures. It was found that the as-prepared catalyst possesses an amorphous structure, which persists at a calcination temperature of 250 °C. After calcination

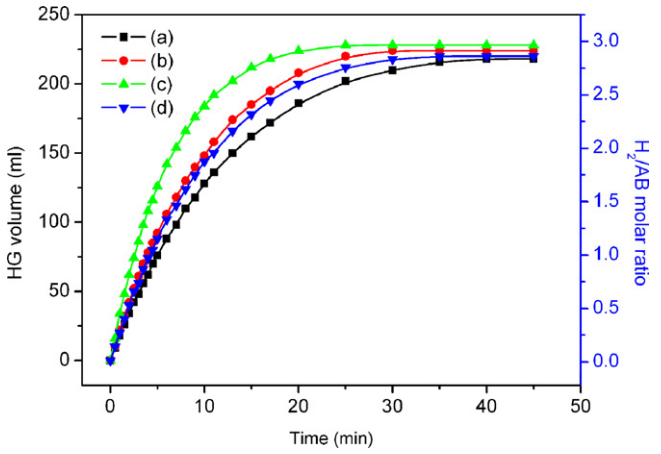

Fig. 2. HG kinetics curves of the AB aqueous solution (10 ml, 1 wt.% AB) at 25 °C in the presence of the as-prepared Co–Mo–B/Ni foam catalyst (1 cm × 1 cm) (a) and those after being calcined at 250 °C (b), 350 °C (c) and 500 °C (d), respectively. The Co–Mo–B loading of catalyst is 16 mg cm^{-2} (Ni foam).

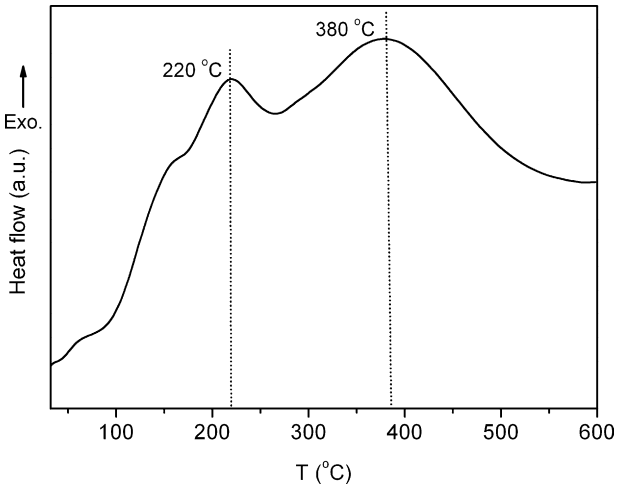

Fig. 4. DSC profile of the Co–Mo–B catalyst. The ramping rate is 10 °C min^{-1}.

of the catalyst at 350 °C for 2 h, the weak and wide diffraction peaks of nanocrystalline Co phase (JCPDS cards 15-0806 and 05-0727) became detectable. By using the Scherrer equation, the average grain size of nanocrystalline Co is roughly estimated to be around 14 nm. Upon further elevating the calcination temperature to 500 °C, the catalyst sample showed intensified diffraction peaks of Co, indicative of the enhanced crystallization degree and increased grain size. As shown in Fig. 4, examination of the as-prepared catalyst by using DSC clearly identified two exothermic effects, which center at 220 and 380 °C, respectively. This finding, together with the XRD results, suggests that crystallization of the Co–Mo–B amorphous alloy proceeds via a two-step process. The amorphous Co–Mo–B catalyst firstly undergoes a structure rearrangement [37,38], followed by precipitation of nanocrystalline Co from the amorphous matrix. Additionally, the as-prepared and post-calcined catalyst samples were also examined by using N_2 adsorption and SEM techniques. Fig. 5 presents the typical BET adsorption isotherms of the catalyst samples, from which the specific surface areas of the as-prepared Co–Mo–B catalyst and that after being calcined at 350 °C were determined to be 4.68 and 4.73 m^2 g^{-1}, respectively. Similarly, the SEM examinations of the series of the catalyst samples did not detect any appreciable change of the surface morphology upon calcination treatment or changing calcination temperature. These findings suggest that the variation of catalytic activity resulting from the calcination treatment should be mainly understood from the subtle structure change. In this regard, better understanding the process and mechanism of precipitation of nanocrystalline Co from the amorphous matrix may provide valuable insight.

Next, we selected the Co–Mo–B/Ni foam catalyst that was calcined at 350 °C for detailed property study, aiming at developing better understanding of the catalytic hydrolysis kinetics of AB. Careful examination of the hydrolysis kinetics curves shown in Fig. 2 find that the HG rate of AB solution gradually decreases with processing the hydrolysis reaction, indicative of non-zero-order hydrolysis kinetics. In our attempt to fit the measurement data using first-order kinetics model, plotting $-\ln(1-C)$ (where C is the conversion of AB) versus reaction time (t) yields a well-fitted straight line, as shown in Fig. 6. This result clearly indicates that, under the applied experimental conditions, the catalyzed hydrolysis of AB follows first-order kinetics with respect to AB concentration. Similar observation was also reported by Mohajeri et al. [19] in their study of the K_2PtCl_6-catalyzed hydrolysis of AB. In contrast, Chandra and Xu [18,26] claimed zero-order hydrolysis kinetics of AB in the presence of supported Pt, Ru, Co and Ni catalysts, whereas Basua et al. [39] reported that the hydrolysis had a fractional reaction order for AB concentration in the presence of Ru/C catalyst on the

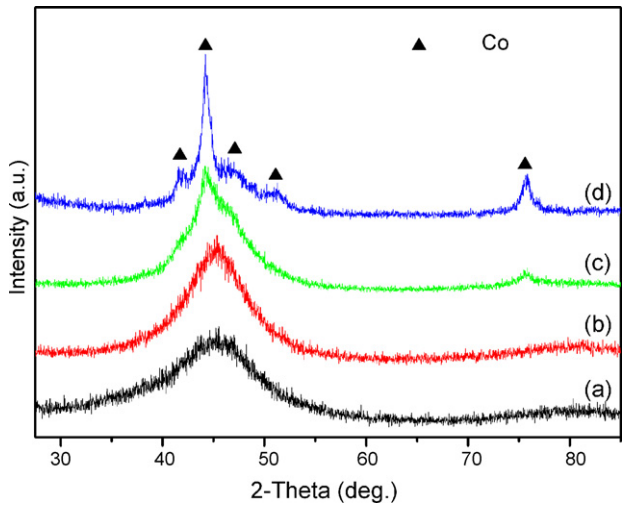

Fig. 3. XRD patterns of the as-prepared Co–Mo–B/Ni foam catalyst (a) and those after being calcined at 250 °C (b), 350 °C (c) and 500 °C (d), respectively.

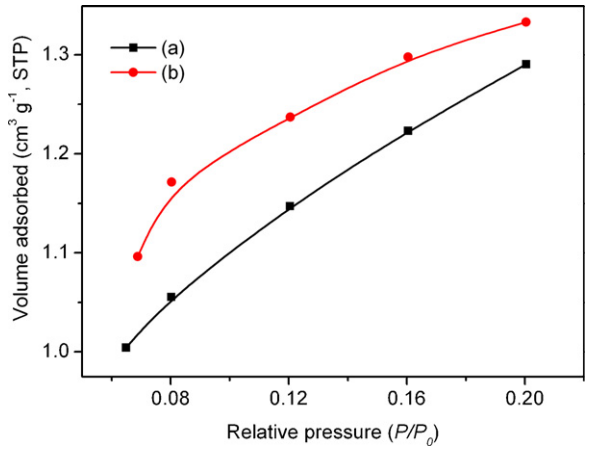

Fig. 5. Nitrogen adsorption isotherms of the as-prepared Co–Mo–B/Ni foam catalyst (a) and that after being calcined at 350 °C (b), respectively.

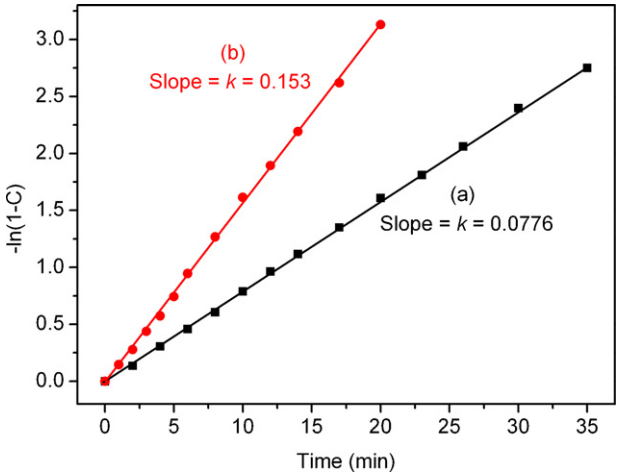

Fig. 6. AB conversion as a function of the hydrolysis reaction time in the presence of the as-prepared Co–Mo–B/Ni foam catalyst (a) and that after being calcined at 350 °C (b).

basis of their experiment study and model analysis. Notably, all the above-mentioned studies involve the usage of dilute AB solutions (≤1 wt.% AB). The possibility of an AB concentration-dependent phenomenon can therefore be precluded. Currently, the distinct divarication on hydrolysis kinetics comes from whether the variation of catalyst species or their relative concentration to AB remains to be checked.

Another set of experiments were carried out to evaluate the effect of catalyst amount on the hydrolysis kinetics of AB. Fig. 7a presents the HG kinetics curves of the aqueous AB solution (10 ml, 1 wt.%) using varied amounts of Co–Mo–B/Ni foam catalyst. It has been found that the HG kinetics becomes apparently favorable with increasing the catalyst amount. In all cases, the hydrolysis reaction is first-order with respect to AB concentration, and the first-order rate constant increases with increasing the catalyst amount. To minimize the measurement error, we selected the initial stage of hydrolysis reaction to determine the hydrolysis rate. This is rationalized by our finding in the relevant $NaBH_4$ hydrolysis reaction system. It was found that the initial stage of the first-order hydrolysis reaction of $NaBH_4$ (for the aqueous solutions containing $NaBH_4$ concentration below the threshold value) can be fairly well described using quasi-zero-order kinetics model [40]. As shown in the inset of Fig. 7a, the HG volume increases linearly with increasing the reaction time at the initial stage of the hydrolysis reaction of AB. Plotting ln(initial HG rate) versus ln(catalyst amount) yields a well-fitted straight line with a slope of 0.962, as shown in Fig. 7b. This result clearly indicates that the catalytic hydrolysis reaction of AB is first-order with respect to catalyst amount.

Fig. 8 presents the catalytic hydrolysis kinetics curves of the AB aqueous solution at temperatures ranging from 25 to 40 °C. As expected, HG rate increases with elevating the solution temperature. In all cases, the hydrolysis of AB was found to obey first-order rate law with respect to the AB concentration. Using the first-order rate constant (k) at varied temperatures, the apparent activation energy of the hydrolysis reaction employing the Co–Mo–B/Ni foam catalyst was determined to be 44.3 kJ mol^{-1} (as shown in the inset of Fig. 8). This value compares favorably with the literature results for Ni–Ag/C (51.5 kJ mol^{-1}) [24] and Co/γ-Al_2O_3 (62 kJ mol^{-1}) [26] catalysts.

Catalyst durability is another important factor that determines its usefulness in the practical HG systems. In the present study, the durability of the Co–Mo–B/Ni foam catalyst was tested by the cyclic hydrolysis experiments. As seen in Fig. 9, the Co–Mo–B/Ni foam catalyst shows satisfactory durability in the cyclic usage. The

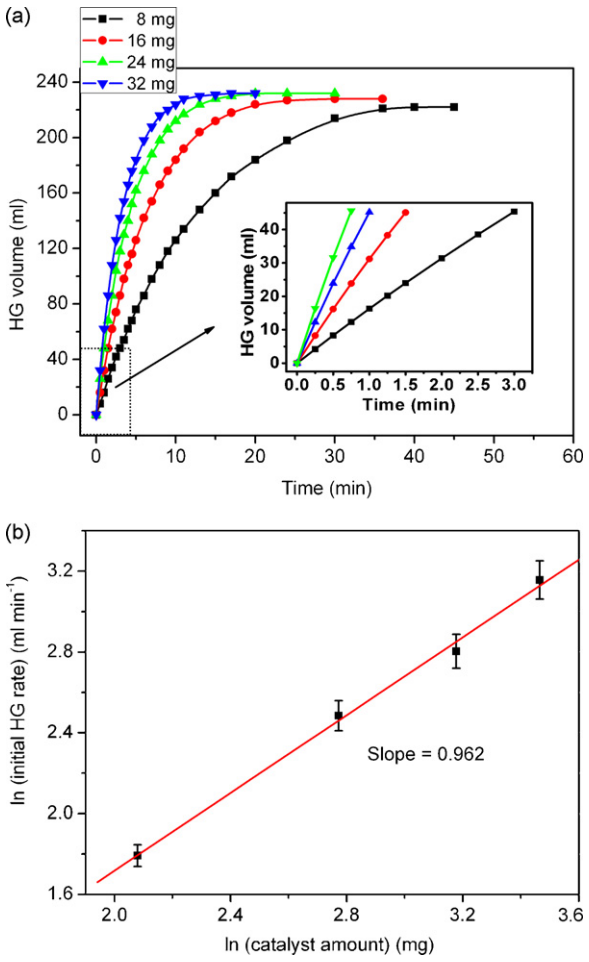

Fig. 7. HG kinetics curves of the AB aqueous solution (10 ml, 1 wt.% AB) at 25 °C in the presence of varied amounts of the Co–Mo–B/Ni foam catalyst that was calcined at 350 °C under Ar atmosphere for 2 h (a). The inset shows the HG volume as a function of reaction time in the initial stage of hydrolysis of AB; (b) depicts the initial HG rate as a function of the catalyst amount.

catalyst at its tenth time usage can still achieve 93% conversion of AB within 23 min at 25 °C, with a catalytic activity only slightly inferior to that in the first cycle. It is believed that, besides the robustness of the catalyst (as seen in Fig. 1b and d), the weak alkaline solution

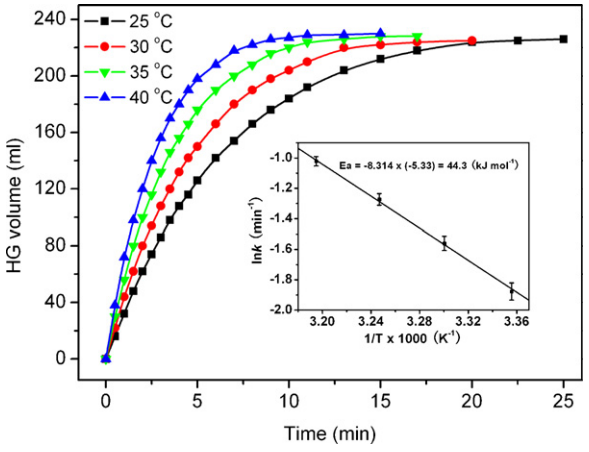

Fig. 8. HG kinetics curves of the AB aqueous solution (10 ml, 1 wt.% AB) at different solution temperatures in the presence of the post-calcined Co–Mo–B/Ni foam catalyst at 350 °C (1 cm × 1 cm, Co–Mo–B loading of 16 mg cm^{-2}). The inset shows the Arrhenius equation treatment of the temperature-dependent first-order rate constant, which determined the apparent activation energy to be 44.3 kJ mol^{-1}.

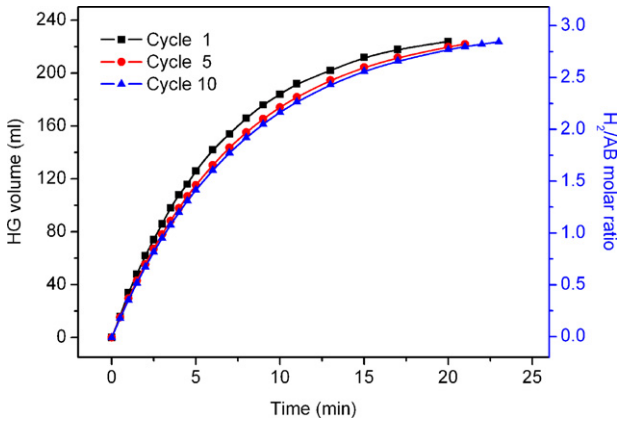

Fig. 9. Cyclic performance of the Co–Mo–B/Ni foam catalyst (calcined at 350 °C for 2 h) in catalyzing the hydrolysis of AB.

environment in the hydrolysis process of AB also contributes to the durability of the catalyst.

The Co–Mo–B/Ni foam catalyst is an effective and robust catalyst for promoting the hydrolysis reaction of AB at ambient temperatures. HG from hydrolysis of AB can be readily switched on/off by controlling the contact/separation of the catalyst with the fuel solution. Furthermore, the AB aqueous solution is non-flammable, nontoxic and highly stable under inert atmosphere, and the hydrolysis by-product (NH_4BO_2) is environmentally benign. The sum of these properties makes the catalyzed AB hydrolysis system promising for hydrogen carrier, particularly for power generation in portable devices that employ proton-exchange membrane cells. However, efficient and cost-effective regeneration of the spent fuel resulting from the hydrolysis of AB is critical to the successful application of AB as a solid hydrogen carrier.

4. Conclusions

We have successfully prepared a cost-effective Co–Mo–B alloy/Ni foam catalyst by using a modified electroless plating method. After being calcined at an optimized condition (at 350 °C under Ar atmosphere for 2 h), the catalyst exhibits high and durable catalytic activity towards the hydrolysis reaction of AB at ambient temperatures. Under our experimental conditions, the hydrolysis of AB in the presence of Co–Mo–B/Ni foam catalyst exhibits first-order kinetics with respect to AB concentration and catalyst amount, respectively, with an apparent activation energy of 44.3 kJ mol^{-1}. Our study illustrates the potential of non-noble transition metal catalysts in developing high-performance chemical hydrogen storage systems.

Acknowledgements

The financial supports for this research from the Hundred Talents Project of Chinese Academy of Sciences, the National High-Tech. R&D Program of China (863 Program, Grant No. 2006AA05Z104), the National Natural Science Foundation of China (Grant No. 50801059), the National Basic Rsearch Program of China (973 program, Grant No. 2010CB631305), and the Frontier Project of CAS Knowledge Innovation Program (Grant No. KGCXZ-YW-342) are gratefully acknowledged.

References

[1] L. Schlapbach, A. Züttel, Nature 414 (2001) 353–358.
[2] S. Orimo, Y. Nakamori, J.R. Eliseo, A. Züttel, C.M. Jensen, Chem. Rev. 107 (2007) 4111–4132.
[3] F.H. Stephens, V. Pons, R.T. Baker, Dalton Trans. 25 (2007) 2613–2626.
[4] T.B. Marder, Angew. Chem. Int. Ed. 46 (2007) 8116–8118.
[5] P. Wang, X.D. Kang, Dalton Trans. 40 (2008) 5400–5413.
[6] C.W. Hamilton, R.T. Baker, A. Staubitz, I. Manners, Chem. Soc. Rev. 38 (2009) 279–293.
[7] M. Chandra, Q. Xu, J. Power Sources 156 (2006) 190–194.
[8] A. Gutowska, L.Y. Li, Y.S. Shin, C.M.M. Wang, X.H.S. Li, J.C. Linehan, R.S. Smith, B.D. Kay, B. Schmid, W. Shaw, M. Gutowski, T. Autrey, Angew. Chem. Int. Ed. 44 (2005) 3578–3582.
[9] D.J. Heldebrant, A. Karkamkar, N.J. Hess, M. Bowden, S. Rassat, F. Zheng, K. Rappe, T. Autrey, Chem. Mater. 20 (2008) 5332–5336.
[10] (a) X.D. Kang, Z.Z. Fang, L.Y. Kong, H.M. Cheng, X.D. Yao, G.Q. Lu, P. Wang, Adv. Mater. 20 (2008) 2756–2760;
(b) Z. Xiong, C.K. Yong, G. Wu, P. Chen, W. Shaw, A. Karkamkar, T. Autrey, M.Q. Jones, S.R. Johnson, P.P. Edwards, W.I.F. David, Nat. Mater. 7 (2008) 138–141.
[11] M. Diwan, V. Diakov, E. Shafirovich, A. Varma, Int. J. Hydrogen Energy 33 (2008) 1135–1141.
[12] (a) C.A. Jaska, K. Temple, A.J. Lough, I. Manners, J. Am. Chem. Soc. 125 (2003) 9424–9434;
(b) C.A. Jaska, I. Manners, J. Am. Chem. Soc. 126 (2004) 9776–9785.
[13] M.C. Denney, V. Pons, T.J. Hebden, D.M. Heinekey, K.I. Goldberg, J. Am. Chem. Soc. 128 (2006) 12048–12049.
[14] M.E. Bluhm, M.G. Bradley, R. Butterick, U. Kusari, L.G. Sneddon, J. Am. Chem. Soc. 128 (2006) 7748–7749.
[15] S.C. Amendola, S.L. Sharp-Goldman, M.S. Janjua, N.C. Spencer, M.T. Kelly, P.J. Petillo, M. Binder, Int. J. Hydrogen Energy 25 (2000) 969–975.
[16] Q. Xu, M. Chandra, J. Alloys Compd. 446/447 (2007) 729–732.
[17] M. Chandra, Q. Xu, J. Power Sources 159 (2006) 855–860.
[18] M. Chandra, Q. Xu, J. Power Sources 168 (2007) 135–142.
[19] N. Mohajeri, A. T-Raissi, O. Adebiyi, J. Power Sources 167 (2007) 482–485.
[20] P.V. Ramachandran, P.D. Gagare, Inorg. Chem. 46 (2007) 7810–7817.
[21] V.I. Simagina, P.A. Storozhenko, O.V. Netskina, O.V. Komova, G.V. Odegova, Y.V. Larichev, A.V. Ishchenko, A.M. Ozerova, Catal. Today 138 (2008) 253–259.
[22] T.J. Clark, G.R. Whittell, I. Manners, Inorg. Chem. 46 (2007) 7522–7527.
[23] F.Y. Cheng, H. Ma, Y.M. Li, J. Chen, Inorg. Chem. 46 (2007) 788–794.
[24] C.F. Yao, L. Zhuang, Y.L. Cao, X.P. Ai, H.X. Yang, Int. J. Hydrogen Energy 33 (2008) 2462–2467.
[25] J.M. Yan, X.B. Zhang, S. Han, H. Shioyama, Q. Xu, Angew. Chem. Int. Ed. 47 (2008) 2287–2289.
[26] Q. Xu, M. Chandra, J. Power Sources 163 (2006) 364–370.
[27] S.B. Kalidindi, M. Indirani, B.P. Jagirdar, Inorg. Chem. 47 (2008) 7424–7429.
[28] S.B. Kalidindi, U. Sanyal, B.P. Jagirdar, Phys. Chem. Chem. Phys. 10 (2008) 5870–5874.
[29] P. Krishnan, S.G. Advani, A.K. Prasad, Appl. Catal. B: Environ. 86 (2009) 137–144.
[30] N. Malvadkar, S. Park, M. Urquidi-MacDonald, H. Wang, M.C. Demirel, J. Power Sources 182 (2008) 323–328.
[31] J. Liang, Y. Li, Y. Huang, J. Yang, H. Tang, Z. Wei, P.K. Shen, Int. J. Hydrogen Energy 33 (2008) 4048–4054.
[32] N. Patel, R. Fernandes, G. Guella, A. Kale, A. Miotello, B. Patton, C. Zanchetta, J. Phys. Chem. C 112 (2008) 6968–6976.
[33] H.B. Dai, Y. Liang, P. Wang, H.M. Cheng, J. Power Sources 177 (2008) 17–23.
[34] H.B. Dai, Y. Liang, P. Wang, X.D. Yao, T. Rufford, M. Lu, H.M. Cheng, Int. J. Hydrogen Energy 33 (2008) 4405–4412.
[35] M.G. Hu, J.M. Van Paasschen, R.A. Geanangel, J. Inorg. Nucl. Chem. 39 (1977) 2147–2150.
[36] I. Lucas, L. Perez, C. Aroca, P. Sánchez, E. López, M.C. Sánchez, J. Magn. Magn. Mater. 290/291 (2005) 1513–1516.
[37] H.X. Li, Y.D. Wu, H.S. Luo, M.H. Wang, Y.P. Xu, J. Catal. 214 (2003) 15–25.
[38] H. Yamashita, T. Funabiki, S. Yoshida, J. Chem. Soc. Chem. Commun. (1984) 868–869.
[39] S. Basua, A. Brockman, P. Gagare, Y. Zheng, P.V. Ramachandran, W.N. Delgass, J.P. Gore, J. Power Sources 188 (2009) 238–243.
[40] H.B. Dai, Y. Liang, L.P. Ma, P. Wang, J. Phys. Chem. C 112 (2008) 15886–15892.